Multifunctional Traceable Liposomes with Temperature-Triggered Drug Release and Neovasculature-Targeting Properties for Improved Cancer Chemotherapy

Multifunctional traceable liposomes with temperature-triggered drug release and neo-vasculature targeting properties for improved cancer chemotherapy

Eiji Yuba[1]*, Munenobu Takashima[1], Takaaki Hayashi[1], Daisuke Kokuryo[2,3], Ichio Aoki[3], Atsushi Harada[1], Sadahito Aoshima[4], Uma Maheswari Krishnan[5], Kenji Kono[1]

[1]Department of Applied Chemistry, Graduate School of Engineering, Osaka Prefecture University, 1–1 Gakuen–cho, Naka–ku, Sakai, Osaka 5998531, Japan

[2]Graduate School of System Informatics, Kobe University, Kobe, Hyogo 6578501, Japan

[3]National Institute of Radiological Sciences, National Institutes for Quantum and Radiological Science and Technology, Chiba 2638555, Japan

[4]Department of Macromolecular Science, Graduate School of Science, Osaka University, Toyonaka, Osaka 5600043, Japan

[5]Centre for Nanotechnology & Advanced Biomaterials, School of Arts, Science & Humanities, and School of Chemical & Biotechnology, SASTRA Deemed-to-be University, Thanjavur 613401, India

***Corresponding Author:** E-mail: yuba@chem.osakafu-u.ac.jp (E. Yuba); Tel: +81-72-254-9330

Abstract

Poor distribution of nanocarriers at the tumor site and insufficient drug penetration into the tissue are major challenges in the development of effective and safe cancer therapy. Here, we aim to enhance the therapeutic effect of liposomes by accumulating doxorubicin-loaded liposomes at high concentrations in and around the tumor, followed by heat-triggered drug release to facilitate low molecular weight drug penetration throughout the tumor. A cyclic RGD peptide (cRGD) was incorporated into liposomes decorated with a thermosensitive polymer that allowed precise tuning of drug release temperature (i.e., Polymer-lip) to develop a targeted thermosensitive liposome (cRGD-Polymer-lip). Compared with conventional thermosensitive liposomes, cRGD-Polymer-lip enhanced the binding of liposomes to endothelial cells leading to their accumulation at the tumor site upon intravenous administration in tumor-bearing mice. Drug release triggered by local heating strongly inhibited tumor growth. Notably, tumor remission was achieved via multiple administrations of cRGD-Polymer-lip and heat treatments. Thus, combining the advantages of tumor neovascular targeting and heat-triggered drug release, these liposomes offer high potential for minimally invasive and effective cancer chemotherapy.

Keywords: liposome, doxorubicin, neovasculature, stimuli-sensitive, MRI

Introduction

Several studies have focused on developing drug delivery systems (DDS) that selectively deliver drugs to the target site and kill cancer cells to achieve highly efficient chemotherapy, while reducing adverse effects on normal tissues. Nanoparticle-based DDS have been extensively investigated, as they are known to accumulate in tumor tissues via the enhanced permeability and retention (EPR) effect, resulting from the enhanced leakiness of blood vessels and premature lymphatic system in the tumor tissue.[1–4]

Although various types of DDS such as liposomes, micelles, and polymeric nanoparticles[5–7] have been developed, only a few DDS, such as anticancer drug-loaded liposomes, have been approved for use in clinical therapeutics. Nanocarriers of size 50–200 nm can accumulate in the tumor tissue passively via the EPR effect.[4] However, as some tumor tissues possess stroma-rich and fibrotic structures, the entry of nanoparticles into deeper regions of tumor tissue is hindered.[8–10] Whereas, low molecular-weight anticancer drugs can penetrate when released within or near tumors. Therefore, innovative strategies are necessary to increase the concentration of nanoparticles in and around the tumor tissue and trigger the release of low molecular-weight anticancer drugs in response to external stimuli, facilitating the dissemination of anticancer drugs deep into the tumor. However, the development of such highly ordered multifunctional DDS remains challenging.

Regulated release of drugs from nanocarriers in response to an external stimulus is a promising strategy[11–17]; for example, thermosensitive liposomes can effectively release drugs in response to externally applied heat.[18–20] Previously, we reported liposomes modified with poly[2-(2-ethoxy)ethoxyethyl vinyl ether-*block*-octadecyl vinyl ether] (p(EOEOVE-*b*-ODVE); Figure 1), which has a lower critical solution temperature (approximately 40 °C).[21,22] p(EOEOVE-*b*-ODVE)-modified liposomes show rapid anticancer drug release above 40 °C because the EOEOVE block becomes hydrophobic and destabilizes the liposomal

membrane.[22] Intravenous administration of these liposomes into colon cancer-bearing mice and subsequent local heat application at the tumor site exerts significant antitumor effects.[21,22]

To promote the accumulation of nanocarriers at the tumor sites, targeting approaches using ligands of tumor- or tumor tissue-specific receptors have been investigated. We previously prepared HER2-specific antibody (Herceptin)-modified liposomes.[23] However, the enhancement in therapeutic effect of Herceptin-modified liposomes was modest compared with liposomes without ligands probably because tumor-specific ligand-modified liposomes could not reach to tumor cells through limited penetration into the dense stromal tissues surrounding blood vessels.[8–10] An alternative strategy to concentrate nanocarriers in the tumor tissue involves neovasculature-targeting using tumor neovasculature-specific ligands. Cyclic RGD peptide (cRGD) is a typical neovasculature-specific ligand. It has a high affinity for the $\alpha_v\beta_3$ integrin expressed on the surface of endothelial cells in tumor neovascular vessels.[24,25] Moreover, cRGD-containing polymeric micelles or liposomes can significantly improve the accumulation of these nanoparticles at the tumor site.[26–28]

Therefore, we aimed to improve the efficacy of nanocarrier-based chemotherapy by combining following three strategies (Figure 1). First, we increased the concentration of doxorubicin-loaded liposomes around the tumor using a neovasculature-targeting cRGD. Second, we incorporated a thermosensitive polymer into the liposomes that is temperature triggered to release doxorubicin and promote penetration into the tumor tissue selectively. Third, to monitor drug accumulation at the tumor site and optimize the heating time frame, we modified the liposomes with a magnetic resonance (MR)-detectable gadolinium chelate moiety (Gd-DOTA) and increased the MR imaging (MRI) sensitivity using a polyamidoamine dendron-bearing lipid[29] (Figure 1). Herein, we evaluated the performance of these multifunctions-introduced liposomes for cancer therapy compared with traditional temperature-sensitive liposomes (TTSL), which are currently undergoing clinical trials.[30]

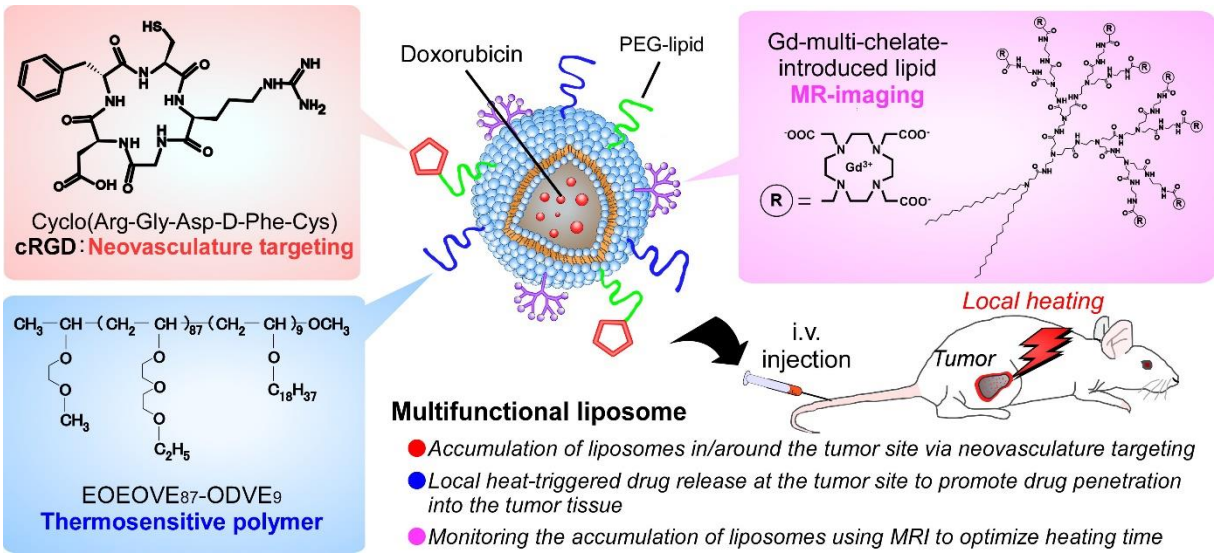

Figure 1. Study design. Multifunctional liposomes for tumor neovasculature-targeting, imaging, and selective drug release under external heat stimulus, thereby achieving highly precise cancer chemotherapy.

Materials and Methods

Materials

Egg yolk phosphatidylcholine (EYPC), 1-palmitoyl-2-stearoyl-*sn*-glycero-3-phosphocholine (HSPC), N-[methoxy (polyethylene glycol) 5000]-distearoyl phosphatidylethanolamine (PEG-PE), and maleimide-terminated poly(ethylene glycol) 2000-distearoyl phosphatidylethanolamine (Mal-PEG-PE) were kindly donated by NOF Co. (Tokyo, Japan). 1,2-Dipalmitoyl-*sn*-glycero-3-phosphocholine (DPPC), cholesterol (Chol), and fetal bovine serum (FBS) were obtained from Sigma-Aldrich (Tokyo, Japan). Cyclo(Arg-Gly-Asp-D-Phe-Cys) (cRGD) was supplied by Synpeptide (Shanghai, China). Doxorubicin (DOX) and 3-(4,5-dimethyl-2-thiazolyl)-2,5-diphenyl-2H-tetrazolium bromide (MTT) were purchased from Wako Pure Chemical Industries Co., Ltd. (Osaka, Japan). Triton X-100 was obtained from Tokyo Chemical Industries Ltd. (Tokyo, Japan). Fluorescent dye 1,1′-dioctadecyl-3,3,3′,3′-tetramethylindocarbocyanine perchlorate (DiI) was obtained from Life Technologies (Carlsbad, CA, USA). p(EOEOVE-*b*-ODVE) was synthesized as previously

described.[21,22] The average molecular weight of p(EOEOVE-*b*-ODVE) was estimated to be 1.0×10^4 using gel permeation chromatography. The average repeating unit of pEOEOVE and pODVE blocks was estimated to be 87 and 9, respectively, using proton nuclear MR (^{1}H NMR). The copolymer was shown to undergo a transition at 40 °C, as estimated by turbidity measurement. Gd-DOTA-conjugated polyamidoamine dendron-bearing lipid was synthesized as previously described.[29]

Preparation of liposomes

A dry, thin membrane comprising a mixture of EYPC, Chol, p(EOEOVE-*b*-ODVE), PEG-PE, and Mal-PEG-PE, in a molar ratio of 50.5:45.4:0.1:2:2, was dispersed in an aqueous solution containing 300 mM ammonium sulfate (pH 5.3) by brief sonication using a bath-type sonicator. The obtained liposome suspension was extruded through a polycarbonate membrane with a pore diameter of 100 nm and centrifuged by ultracentrifugation (163,383 × *g*, 1 h, 4 °C). The liposome pellet was dispersed in PBS (pH 7.4) to form a pH gradient. Next, aqueous DOX solution (10 mg/mL) was added to the liposome suspension at a DOX/lipid (g/mol) ratio of 75:1, and the mixed solution was incubated for 1 h at 30 °C. Free DOX was removed using repeated ultracentrifugation (163,383 × *g*, 1 h, twice) at 4 °C. cRGD solution (1 mg/mL) was added to the liposome suspension at 0.04 eq. to the total lipid (moles) and incubated overnight at 4 °C to allow the thiol group in the cysteine residue of cRGD to react with the maleimide group in liposomes. Unconjugated cRGD was removed using repeated ultracentrifugation (163,383 × *g*, 1 h, twice) at 4 °C. The obtained liposome suspension was stored at 4 °C until further analyses.

Preparation of TTSL and conjugation of cRGD were performed as described above using a representative lipid composition of TTSL: DPPC, HSPC, Chol, PEG-PE, and Mal-PEG-PE in a molar ratio of 54:27:15:2:2.[31]

Characterization of liposomes

Lipid concentration was determined using the Wako Phospholipid C assay (Wako Pure Chemical Industries Co., Ltd.). The efficiency of encapsulation of DOX by liposomes was estimated by measuring the absorbance of DOX at 499 nm for the liposomes dissolved in 0.3 M HCl (50 vol%)-ethanol (50 vol%) before and after purification by ultracentrifugation. The amounts of cRGD in liposomes were determined using the MicroBCA Protein Assay kit (Thermo Fisher Scientific, Waltham, MA, USA). Lipid-derived absorbance using liposomes without cRGD was subtracted to calculate the amount of peptide on the liposomes. Diameters of the liposomes (0.1 mM of lipid concentration) were measured using a Zetasizer Nano ZS (Malvern Instruments Ltd., Worcestershire, UK). Data were obtained as the mean of more than three independent measurements of different samples.

Analysis of drug release from liposomes

DOX-loaded liposomes (final lipid concentration: 13.3 μM) were added to PBS containing 50% FBS at a given temperature and emission signal of the mixed suspension was obtained at 590 nm upon excitation at 468 nm using a spectrofluorometer (FP-6500 or FP-8500; Jasco, Tokyo, Japan). The percent release of DOX from liposomes was defined as:

$$\textbf{Release}\ (\%) = (\boldsymbol{F_t} - \boldsymbol{F_i})/(\boldsymbol{F_f} - \boldsymbol{F_i})\ \times \mathbf{10}$$

where F_t and F_f denote the intermediary and final fluorescence intensities, respectively, of the suspension at a given temperature. F_f was obtained as the fluorescence intensity of the liposome suspension after the rupture of liposomes by addition of 10% Triton X-100 solution (30 μL). As DOX was released very quickly at temperature above 40 °C, it was challenging to estimate the initial fluorescence intensity of the DOX-loaded liposome suspension. Fluorescence intensity of the suspension at 10 °C was considered the initial intensity because the release of DOX was negligible at this temperature, and the DOX fluorescence was strongly quenched.

Analysis of cell-liposome interactions

Liposomes containing DiI were prepared as described earlier, except that a mixture of polymer and lipids containing DiI (0.6 mol%) was dispersed in PBS. The F-2, a murine endothelial cell line, or colon26, a murine colon cancer cell line, cells were cultured (5×10^4 cells) in Dulbecco's Modified Eagle Medium (DMEM) or Roswell Park Memorial Institute Medium (RPMI)-1640 supplemented with 10% FBS and antibiotics overnight in a 24-well plate. The cells were washed twice with PBS and incubated in the culture medium (0.45 mL). DiI-labeled liposomes of various lipid concentrations (0.05 mL) were added gently to the cells and incubated for 4 h at 37 °C. After incubation, the cells were washed thrice with PBS. The mean fluorescence intensities of these cells were determined using flow cytometry (CytoFlex; Beckman Coulter, Inc., Brea, CA, USA).

For analyzing the intracellular distribution of liposomes, F-2 cells (2×10^5) were cultured overnight in a glass-bottom dish and washed twice with PBS. Next, the cells were incubated in the culture medium (1 mL). DiI-labeled liposomes (0.32 mM lipid concentration, 1 mL) were added gently to the cells and incubated for 4 h at 37 °C. After incubation, the cells were washed thrice with PBS and visualized with a confocal laser scanning microscopy (LSM5 EXCITER; Carl Zeiss, Oberkochen, Germany).

Analysis of cytotoxicity of DOX-loaded liposomes

F-2 or colon26 cells (2×10^4 cells) were cultured overnight in a 48-well plate and washed with PBS twice, followed by incubation in DMEM or RPMI-1640 supplemented with 10% FBS and antibiotics. Varying amounts of DOX-loaded liposomes were gently added to the cells and incubated for 24 h. The cells were then washed with PBS twice, incubated at 45 °C for 5 min, and subsequently incubated at 37 °C for 24 h. Their viability was evaluated using the MTT assay.

Mice

Seven-week-old female BALB/c mice were purchased from Oriental Yeast Co., Ltd. (Tokyo, Japan). All animal experiments were approved by the Institutional Animal Experimentation Committee of Osaka Prefecture University (approval no. 26-29, 27-95, and 28-119) and performed in compliance with the institutional guidelines for animal care and use.

MRI

Gd-DOTA-conjugated polyamidoamine dendron-conjugated lipid was incorporated into the liposomes as a lipid component (10 mol% of the total lipids). Colon26 cells (1.0×10^6 cells/mouse) were subcutaneously injected into the upper left hind limbs of BALB/c nude mice (7–9 weeks old, female; Japan SLC Inc., Shizuoka, Japan) under anesthesia using isoflurane (1.0–2.0%; Escain, Mylan, PA, USA). When tumor volume exceeded 200 mm^3 (7–14 d after transplantation), *in vivo* MRI was performed using a 7.0 Tesla 40-cm bore magnet (Kobelco and Jastec, Kobe, Japan) interfaced with an Avance I system (Bruker-Biospin, Ettlingen, Germany) with a 35-mm diameter volume coil (Rapid Biomedical, Lymper, Germany). Furthermore, MR images were continuously obtained before and after administering liposomes via the tail vein. Contrast-enhanced T_1-weighted images of tumor mice were acquired using a spin-echo sequence with the following parameters: TR/TE = 400/9.57 ms; Field of view (FOV) = 44.8×44.8 mm^2; matrix = 256×256; resolution = 150 mm × 150 μm; slice thickness = 1.0 mm; and number of acquisitions = 4. The scanning time was 6 min 49 s. During the *in vivo* MRI analyses, rectal temperatures of the mice were monitored using an optical fiber thermometer (FOT-M; FISO Technology, Quebec, Canada) and maintained at approximately 36.5 ± 0.5 °C using warm air produced by a homemade automatic heating system based on an electric temperature controller (E5CN; Omron, Kyoto,

213 Japan). The mice were anesthetized with 1.5–2.0% isoflurane (Escain) gas and a 1:2 O_2:
214 room-air mixture.
215
216 **Analysis of *in vivo* antitumor effects of DOX-loaded liposomes**
217 Colon26 tumor-bearing mice were prepared as described above. When the tumor
218 volume exceeded 150 mm^3, mice were intravenously injected with DOX-loaded liposomes at
219 a dose of 6 mg kg^{-1} under anesthesia. At 8 h after the injection, the tumor was locally heated
220 at 43 °C for 10 min using a radiofrequency oscillator (RF-hyperthermia HEH-100; Omron).
221 The tumor volumes were determined as follows,
222 $$\mathbf{Volume} = \boldsymbol{L} \times \boldsymbol{W^2}$$
223 where *L* is the longest dimension parallel to the skin surface, and W is the dimension
224 perpendicular to *L* and parallel to the surface. Mice were sacrificed when tumor volumes
225 exceeded 2,000 mm^3. All treated and control (PBS-injected) groups contained 4–5 mice.
226
227 **Statistical analysis**
228 Significant differences between the experimental groups were determined using GraphPad
229 Prism software (v8; GraphPad Software Inc., La Jolla, CA, USA). When one-way ANOVA
230 followed by Tukey's honestly significant difference post hoc test was used, the variance
231 between groups was found to be similar by the Brown-Forsythe test. For single comparisons,
232 a two-tailed Student's *t*-test was used. A log-rank test was employed for analyzing mouse
233 survival. The symbols *, **, and *** indicate *P*-values less than 0.05, 0.01, and 0.001,
234 respectively.
235
236 **Results and Discussion**
237 **Preparation of liposomes**

Thermosensitive polymer-modified liposomes (Polymer-lip) were prepared by hydration of a mixture of the thermosensitive polymer p(EOEOVE-*b*-ODVE) and lipids via hydrophobic interactions of the ODVE segment with the liposomal membrane. Liposomes without the thermosensitive polymers (Lip) and TTSL were prepared as described earlier[31–33] for comparison. Poly(ethylene glycol) (PEG)-lipids were also incorporated into the liposomes to enhance their biocompatibility. Maleimide group-terminated PEG-lipid, Mal-PEG-PE, was used for conjugating cRGD peptide. After purification, almost half of the maleimide groups were modified with cRGD, the contents of which were determined using the MicroBCA assay (Table S1). The anticancer drug DOX (doxorubicin hydrochloride salt) was encapsulated by the liposomes via a pH gradient method. As shown in Table S1, the DOX-loading efficiencies of the five kinds of liposomes were 88.0–97.4%. The size of liposomes determined by dynamic light scattering measurements was 130–160 nm, which was within the suitable range for the EPR effect.[2,4]

Evaluation of liposomes on temperature-dependent drug release

Next, temperature-dependent drug release behaviors of the two liposomes were investigated. Figure 2A shows the kinetics of DOX release from liposomes at 37 °C and 45 °C in the presence of 50% serum. Lip showed negligible DOX release at both 37 °C and 45 °C, whereas Polymer-lip exhibited immediate DOX release at 45 °C. Figure 2B shows the temperature-dependent DOX release after 10 min incubation. Below 37 °C, Polymer-lip showed less than 5% DOX release; however, DOX release was enhanced above 41 °C and reached 90% at 45 °C. Differential scanning calorimetric (DSC) studies showed that in the case of Polymer-lip, initiation of the endothermic transition phase occurred at 38 °C. Additionally, a large peak at 40 °C and a broad endothermic peak up to approximately 50 °C were observed (Figure S1). These indicated initiation of phase transition of pEOEOVE segments on the liposome at 38 °C and subsequent substantial changes in the polymer

conformation at approximately 40 °C.[21,22] Such conformational changes, along with polymer dehydration, could promote interactions between the hydrophobic polymer and liposomal membrane, resulting in DOX leaking from liposomes at temperatures above 38 °C. The DOX release profile of cRGD-Polymer-lip was identical to that of Polymer-lip (Figure 2), indicating that cRGD functionalization at the terminus of the PEG-lipid did not affect the interaction of pEOEOVE with the liposomal membrane. Figure S2 shows the DOX release behavior of TTSL. Although TTSL was found to strongly retain DOX below 40 °C, a sudden release of DOX was observed above 42 °C, which peaked at 44 °C. The drug release profiles corroborated with the DSC profile for TTSL (Figure S1). The gel-to-liquid crystalline transition of the lipid bilayer at 44 °C resulted in the release of DOX from the liposome because membrane permeability was enhanced during the phase transition.[32,33]

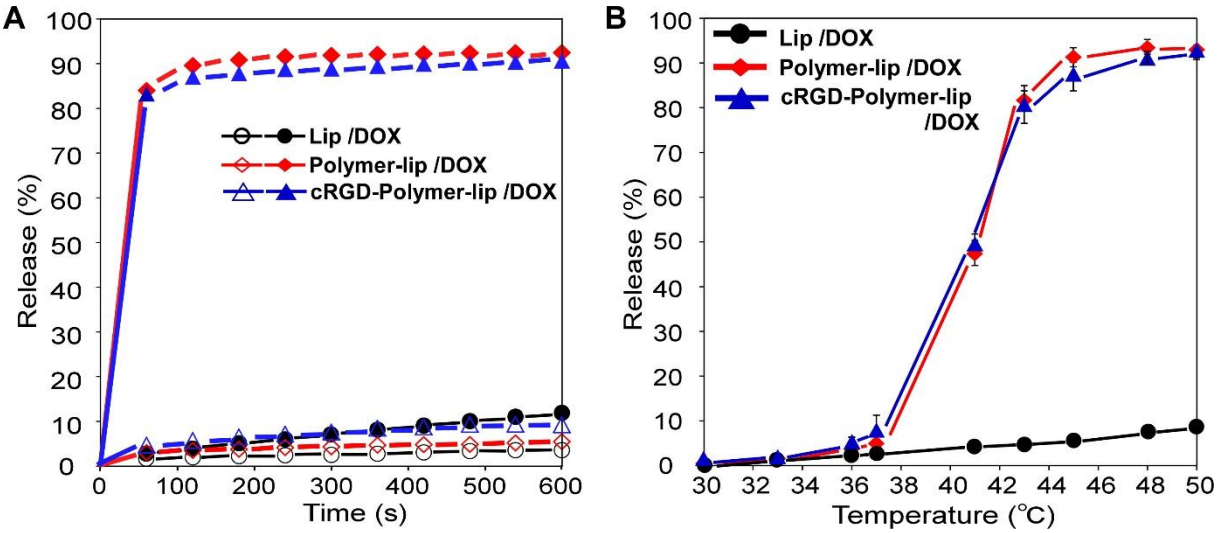

Figure 2. Temperature-triggered drastic drug release from liposomes. (A) Time-resolved DOX release profiles. The open and filled symbols indicate the DOX release profiles at 37 °C and 45 °C, respectively. (B) Temperature-dependent DOX release profiles after 10 min of incubation with DOX-loaded liposomes without thermosensitive polymer (Lip, black), DOX-loaded liposomes with thermosensitive polymer pEOEOVE (Polymer-lip, red), and cRGD-functionalized Polymer-lip (cRGD-Polymer-lip, blue). Data are presented as the mean ± SEM of three experimental replicates.

Interaction of liposomes with cells and cytotoxicity

The effects of cRGD modification on interactions between the liposomes and cells were evaluated using F-2 cells and colon26 cells, which are models of endothelial cells with $\alpha_v\beta_3$ integrin[34] and cancer cells with fewer integrins, respectively. In fact, immunofluorescence analysis revealed that expression level of $\alpha_v\beta_3$ integrin on F-2 cells was significantly higher than that of colon26 cells (Figure S3). DiI-labeled liposomes were added to these cells, and the fluorescence intensity of the cells, resulting from interactions with the liposomes, was measured using a flow cytometer (Figure 3A). After treatment with Polymer-lip, both F-2 and colon26 cells showed similar fluorescence intensities irrespective of the lipid concentration. In F-2 cells, the cRGD-Polymer-lip treatment led to a significantly higher cellular fluorescence than that by treatment with Polymer-lip. However, in colon26 cells, treatment with either of the liposomes showed no significant difference in fluorescence intensities (Figure 3A). Furthermore, when F-2 cells were treated with cRGD-Polymer-lip, bright fluorescence spots were seen in the cells, while no fluorescence signal was found in cells treated with Polymer-lip (Figure 3B). The same trend was observed in the flow cytometric analysis of TTSL and cRGD-TTSL (Figure S4). These results indicated that cRGD modification enhanced the cellular uptake of liposomes via recognition by $\alpha_v\beta_3$ integrin.

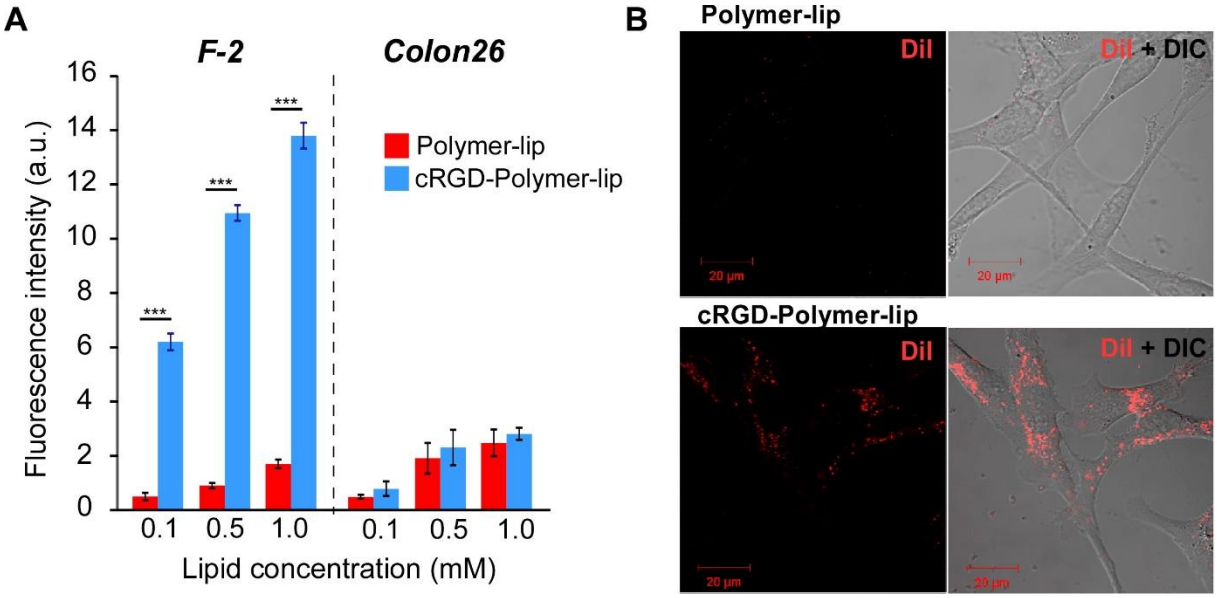

Figure 3. cRGD modification highly improves the cellular association of liposomes. (A) Mean fluorescence intensities of F-2 and colon26 cells treated with DiI-labeled thermosensitive polymer-modified liposomes with or without cRGD (Polymer-lip and cRGD-Polymer-lip, respectively). The cells were incubated with liposomes (0.1, 0.5, or 1.0 mM of lipid concentrations) for 4 h at 37 °C. Data are presented as the mean ± SEM of three experimental replicates. Statistical analyses were performed using a two-tailed Student's *t*-test: ***$P < 0.001$. (B) Confocal laser scanning microscopy images of F-2 cells treated with DiI-labeled liposomes with or without cRGD for 4 h at 37 °C.

Next, *in vitro* cytotoxicity of DOX-loaded liposomes (Polymer-lip and cRGD-Polymer-lip) was investigated. F-2 cells were incubated with the liposomes at varying DOX concentrations, followed by incubation at 45 °C for 5 min to induce DOX release from the liposomes. Polymer-lip and cRGD-Polymer-lip showed negligible cytotoxicity, thus indicating negligible DOX release when cultured at 37 °C (without heat) (Figure 4A). In contrast, 5-min heating at 45 °C decreased cell viability at DOX concentrations greater than 10 μg mL^{-1}. In addition, cRGD-Polymer-lip showed higher cytotoxicity than Polymer-lip. Treatment of free DOX induced high cytotoxicity to F-2 cells irrespective with heat

application compared with DOX-loaded liposomes (Figure 4B). This data is reasonable because free DOX can directly penetrate cell membrane and reach the nucleus via diffusion, which processes was not affected by heat application. For further confirmation of heat-triggered DOX release within the cells, DOX fluorescence from the F-2 cells with or without heat application was observed (Figure S5). The location of cRGD-Polymer-lip within the cells was visualized by the labeling of liposomal membrane using NBD-PE. Many green fluorescence dots were observed from the cells irrespective with heat application, indicating that cRGD-Polymer-lip was internalized within the cells via endocytosis. In the case of no heat application, weak DOX-derived fluorescence spots were seen, resulting from quenching of DOX fluorescence when encapsulated within the liposomes. In contrast, significant increase in DOX fluorescence was observed after heat application. These results suggested that cRGD facilitated high internalization (Figure 3B), and heat-triggered DOX release (Figure S5) could synergistically induce enhanced cytotoxicity against F-2 cells. We also evaluated cytotoxicity against cancer cells (colon26 cells) as same with Figure 4. As shown in Figure S6, heat application significantly increased cytotoxicity of both Polymer-lip and cRGD-Polymer-lip. However, there is no difference between these two liposomes, which corresponds that no significant difference was observed in cellular association of liposomes with or without cRGD (Figure 3A). Therefore, DOX-loaded thermosensitive liposomes with heat can induce the cytotoxicity against both endothelial cells and cancer cells, whereas cRGD modification selectively increased the cytotoxicity against endothelial cells. Cytotoxicity of DOX-loaded TTSL was also evaluated (Figure S7). TTSL did not exhibit any cytotoxicity against F-2 cells under experimental conditions, probably because of its poor interaction with F-2 cells (Figure S4). However, cRGD-TTSL treatment decreased cell viability at the highest DOX concentration at 37 °C, suggesting that increased cellular uptake of cRGD-TTSL induced partial DOX leakage within the cells via degradation at endosomes

or lysosomes at 37 °C. Heating of cRGD-TTSL-treated cells resulted in enhanced drug cytotoxicity.

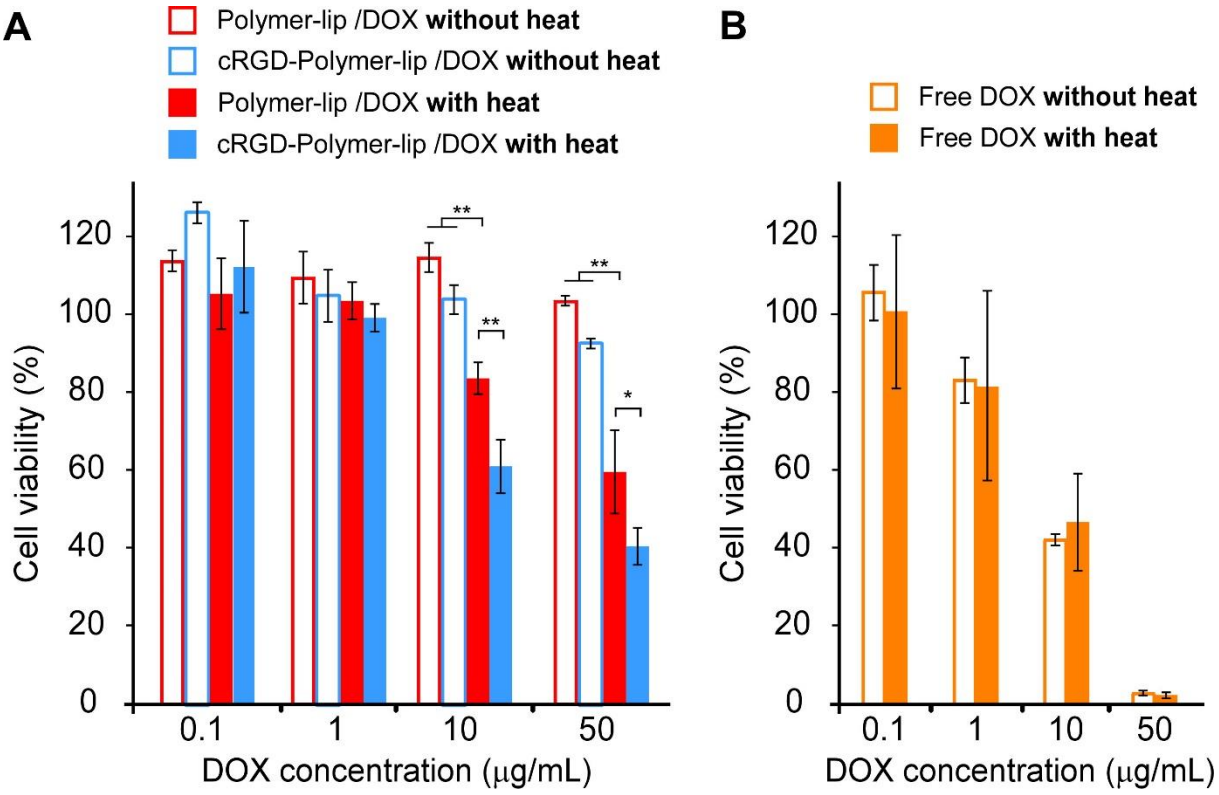

Figure 4. Temperature-triggered drug release effectively kills endothelial cells. Cytotoxicity of (A) DOX-loaded thermosensitive polymer-modified liposomes with or without cRGD (Polymer-lip and cRGD-Polymer-lip, respectively) and (B) free DOX. F-2 cells were incubated with liposomes or free DOX in DMEM supplemented with 10% FBS for 24 h at 37 °C. The cells were subjected to 5-min heat treatment at 45 °C, and the cell viability was measured after 24 h culture. Empty and filled bars indicate cell viability without and with heat treatment, respectively. Data are presented as the mean ± SEM of three experimental replicates. Statistical analyses were performed using one-way ANOVA with Tukey's test: $*P < 0.05$ and $**P < 0.01$.

In vivo performance of liposomes

Monitoring the accumulation of liposomes at the target site is important to evaluate the performance of DDS and optimize its molecular design. Specifically, optimizing the heating

time is crucial for maximizing the therapeutic effect of thermosensitive liposome-based cancer treatments. Among various imaging modalities, MRI has many advantages, such as high spatial resolution (50–100 μm), three-dimensional imaging, no exposure to harmful radiation, and multi-mode imaging (morphology, angiography, perfusion, and metabolism). In this study, we incorporated an MR-detectable gadolinium multi-chelate-conjugated lipid into Polymer-lip and cRGD-Polymer-lip to enable MRI analysis.[29] As the gadolinium multi-chelate-conjugated lipid has eight Gd-DOTA moieties in one lipid molecule, the lipid can introduce sufficient MRI properties without decreasing the DDS performance of thermosensitive liposomes.[25] Liposomes with 10 mol% gadolinium multi-chelate-conjugated lipid were intravenously injected into tumor-bearing mice, and the time-dependence of MR signals at the tumor site was monitored (Figure 5). The MR signal at the tumor site increased with time for both Polymer-lip and cRGD-Polymer-lip. Furthermore, MR signals in cRGD-Polymer-lip-treated mice were higher than that in Polymer-lip-treated mice, thereby suggesting high accumulation of cRGD-Polymer-lip at the tumor site via interaction with the endothelial cells of tumor neovasculature. In cRGD-Polymer-lip-treated mice, markedly high contrast spots appeared at the center of the tumor, and over time, the high-signal area spread across most of the tumor area (Figure 5A). Figure 5C shows time-dependent changes in the MR signal intensity at the tumor site. In both treatment groups, the MR signal markedly increased after injection for up to 3 h and reached a plateau. Moreover, treatment with cRGD-Polymer-lip resulted in MR signal intensity twice as high as that observed with Polymer-lip treatment. In our previous report, Polymer-lip exhibited almost comparable pharmacokinetic property with PEG-liposome, which is a golden standard for EPR effect.[22] Therefore, cRGD modification would provide the neovascular active targeting property to Polymer-lip that intrinsically has a passive targeting property via EPR effect. Figure S8 depicts *ex vivo* fluorescence intensity of liver, spleen and tumor from the mice treated with indocyanine green (ICG)-loaded Polymer-lip or cRGD-Polymer-lip at 24 h after intravenous injection. cRGD-

Polymer-lip showed higher intensity at the tumor than that of Polymer-lip, indicating that cRGD modification could increase not only liposomal accumulation, but also accumulation of liposomal contents to the tumor. For further confirmation of tumor accumulation by cRGD modification, tumor sections were stained with tumor vessel marker (CD31) after intravenous injection of DiI-labeled liposomes with or without cRGD. As shown in Figure S9, cRGD modification apparently increased DiI fluorescence within tumor. In addition, DiI fluorescence derived from liposomes modified with cRGD is likely to be overlapped with CD31-derived fluorescence, suggesting that cRGD-modified liposomes accumulate near tumor vessels.

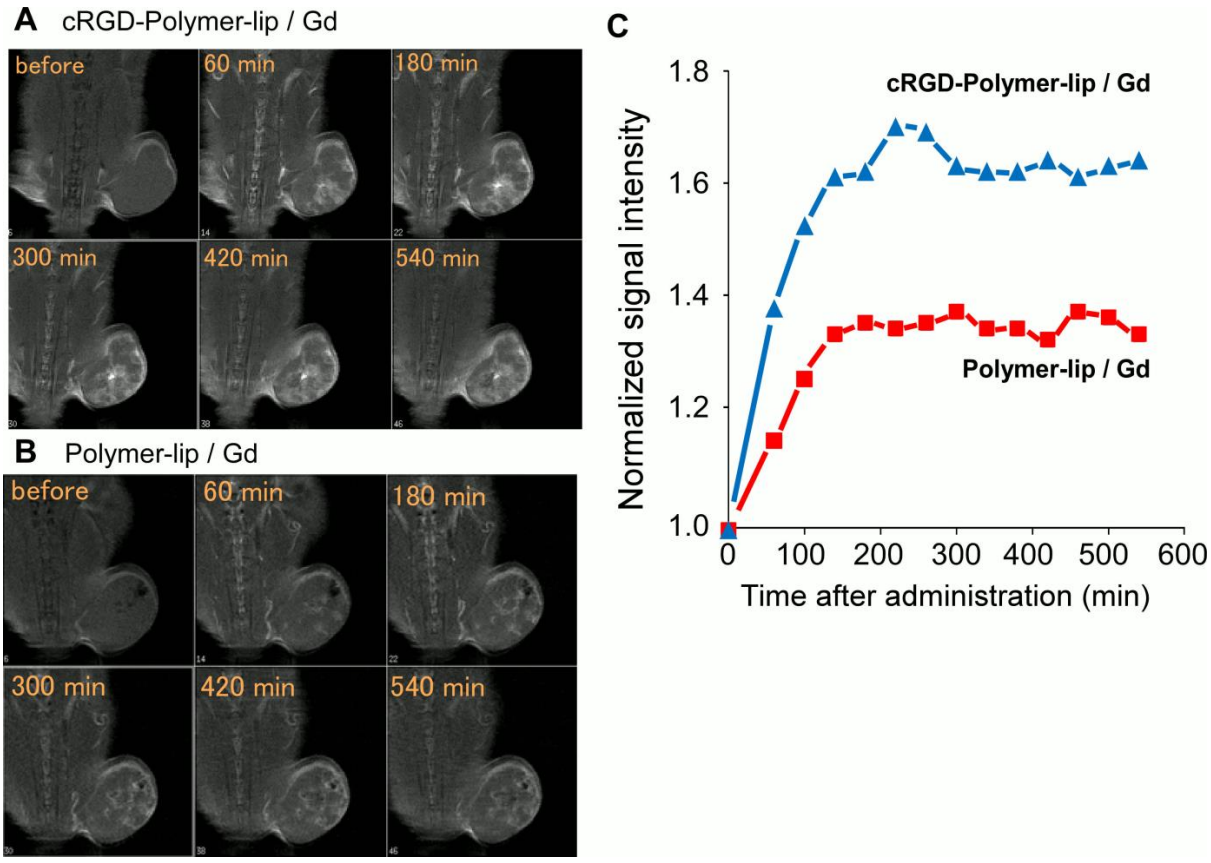

Figure 5. cRGD modification improves tumor accumulation and spreading of liposomes. T_1-weighted images of colon26 tumor-bearing BALB/c nude mice at different time points before and after injection of Gd-DOTA-DL-modified thermosensitive liposomes with (A) or

without (B) cRGD. (C) Normalized signal intensity at the tumor site in the liposome-injected mice, as a function of time.

Considering the high accumulation and spreading profiles of cRGD-Polymer-lip at the tumor site, the antitumor effects of the thermosensitive liposomes were examined. DOX-loaded liposomes were intravenously administered to tumor-bearing mice. Eight hours after injection, during which the liposomes accumulate and spread within tumor (Figure 5A), the tumor site in half the mice was locally heated at 43 °C, a temperature setting used in mild hyperthermia procedures in a clinic, for 10 min and tumor growth was monitored. Figure 6A shows the changes in the relative tumor volume after treatment with Polymer-lip or cRGD-Polymer-lip and with or without heat application. Compared with saline-treated mice, both Polymer-lip- and cRGD-Polymer-lip-treated mice showed slightly suppressed tumor growth even without any heat treatment. Interestingly, local heating of the tumor site was found to significantly suppress tumor growth and extend mouse survival (Figure 6A, 6C). In addition, cRGD-Polymer-lip with heat treatment showed a greater antitumor effect than that by Polymer-lip. Considering that these liposomes with heat can induce the cytotoxicity against both endothelial cells and cancer cells, whereas cRGD modification selectively increased the cytotoxicity against endothelial cells (Figures 4A and S6A), cRGD-Polymer-lip treatment might mainly enhance the cytotoxicity against endothelial cells within tumor tissues. This causes the deletion of nutrient-supplying blood vessels, leading to the promotion of tumor cell death. Besides, in our previous studies, we found that the liposomal contents, released after local heating, effectively penetrate the whole tumor tissue area.[35,36] Therefore, a substantial increase in the accumulation of liposomes at the tumor and spreading within tumor facilitated by cRGD modification (Figure 5A, 5C) might produce efficient penetration of the low molecular-weight anticancer drugs throughout the tumor tissue following their triggered release from the liposomes by local heating. Taking advantage of the tumor neovasculature-

specific accumulation and triggered release, this combination would synergistically improve the antitumor properties of cRGD-Polymer-lip. We further performed the antitumor effect of liposome having conventional active targeting strategy. Polymer-lips modified with or without Transferrin, which is a typical ligand for Transferrin receptor overexpressing on tumor cells, were prepared. As shown in Figure S10, both Polymer-lip and Tf-Polymer-lip showed high antitumor effects in combination with heat treatment, whereas Tf-Polymer-lip induced almost same or slightly weak antitumor effect compared with Polymer-lip. This result suggests that Tf-Polymer-lip could not sufficiently show its tumor cell targeting property probably because of limited penetration of liposomes within tumor tissue after accumulation via EPR effect. These result and speculation further support the importance and the advantage of neovasculature targeting via cRGD towards enhancement of antitumor effects.

We also compared the antitumor activity of cRGD-Polymer-lip with that of cRGD-TTSL (Figure S11). As expected, injection of cRGD-Polymer-lip and cRGD-TTSL only slightly suppressed tumor growth compared with the PBS treatment in the absence of heating. However, local heating significantly increased the antitumor effects of these liposomes. Following heat treatment, the antitumor properties of both cRGD-Polymer-lip and cRGD-TTSL were found to be almost identical. Considering that the temperature range of Polymer-lip for substantial drug release is relatively broad compared with that of TTSL (Figure 2B, Figure S2), Polymer-lip might be able to induce anticancer drug release even at insufficiently heated tumor sites. Furthermore, the thermosensitive properties of Polymer-lip can be adjusted by changing the chemical structure of the thermosensitive polymer. Such characteristics of Polymer-lip would be beneficial in practical clinical scenarios for treating large tumors that are difficult to heat uniformly.

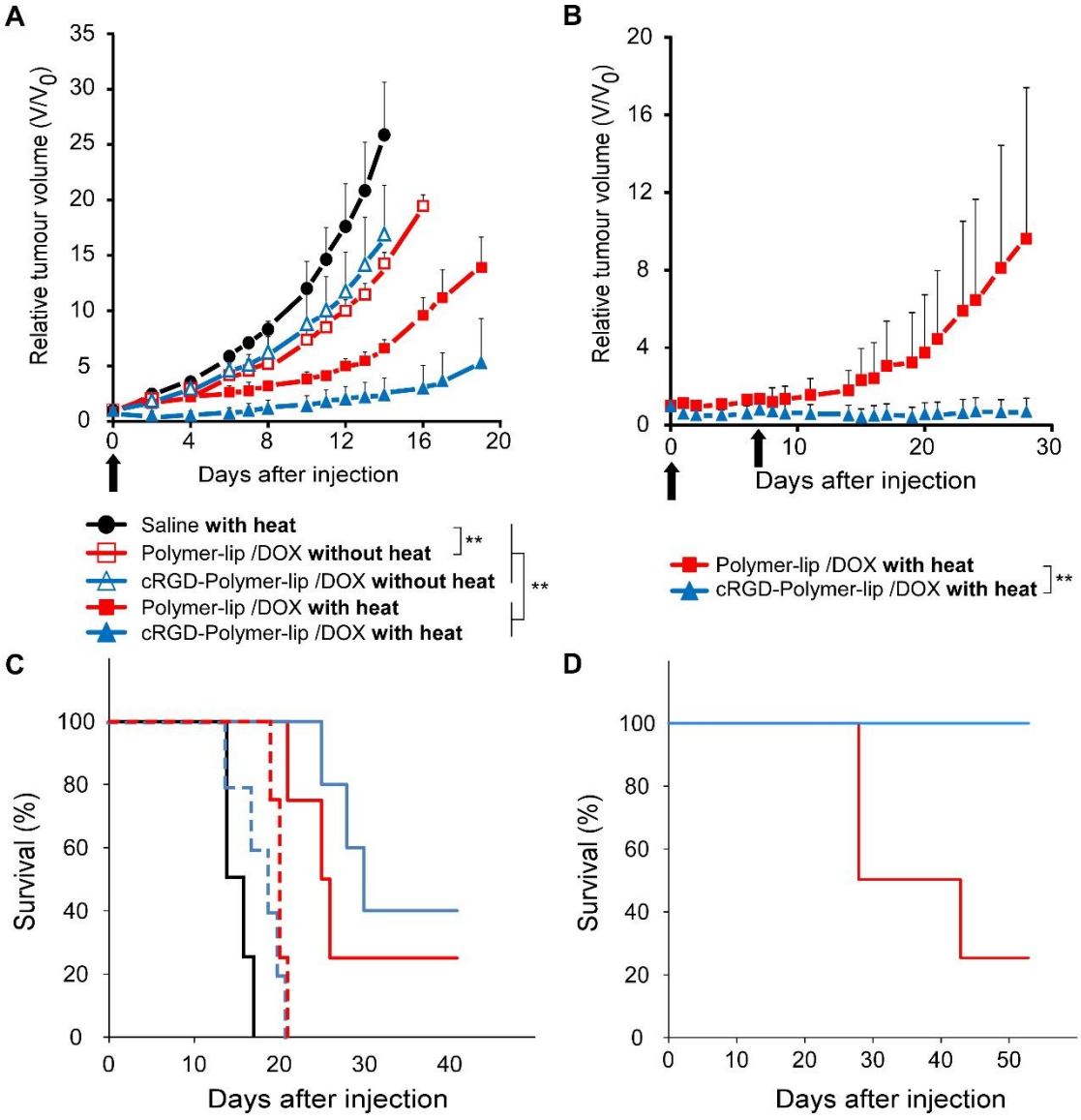

Figure 6. A combination of cRGD modification and temperature-triggered drug release achieves remission of a solid tumor. Change in relative tumor volume (A, B) and mouse survival (C, D) after injection of saline (black circle) or DOX-loaded thermosensitive liposomes with (blue triangle) or without cRGD (red square). Empty and filled symbols represent absence and presence of heat treatment (10 min local heating at 43 °C), respectively. DOX dosage was 6 mg kg^{-1} body weight. Single treatment at 0 d (A, C); treatments at 0 and 7 d (B, D). Black arrows in (A) and (B) indicate sample injection. Dotted lines in (C) indicates treatment without heat application. Data in (A) and (B) are presented as the mean ± SEM. All groups contained 4–5 mice. Mouse survival was analyzed using a log-rank test. $^{**}P < 0.01$.

Complete cure of established tumor by repeated liposome treatment

Single treatment with cRGD-Polymer-lip and local heating stopped the tumor growth temporarily, but the tumor volume started to increase after 8–10 d (Figures 6A and S11). Therefore, the effect of repeated treatment was investigated (Figure 6B, 6D). Liposome injection and local heat application were performed twice at an interval of one week. As shown in Figure 6B, the antitumor effect in the Polymer-lip group improved to some extent after a single treatment, but significant tumor growth was observed after 20 d. Surprisingly, in the cRGD-Polymer-lip-treated group, tumor growth was completely stopped with no recurrence (Figure 6D). As tumor recurrence begins with tumor cell clustering and active angiogenesis,[37] neovasculature targeting by cRGD during the second administration might be effective in attacking the endothelial cells in the neovasculature of tumor cell clusters, leading to destruction of nutrient-supplying blood vessels to tumor. Furthermore, effective penetration of anticancer drugs under local heating could induce tumor cell killing in deep sites of the tumor,[35,36] resulting in a dramatic therapeutic effect without tumor recurrence. Thus, cRGD-conjugated thermosensitive liposomes were highly effective in inducing remission of established solid tumors.

Although cRGD-Polymer-lip showed a remarkable therapeutic effect in the colon cancer-bearing mouse model, there may be limitations in its mechanism of action on therapeutic effect and therapy translation due to substantial differences between mouse tumor models and human cancer. Furthermore, the tumors in the mouse model may not be as heterogenous as the naturally arising tumors in humans. Thus, further investigation of cRGD-Polymer-lip accumulation behavior, small molecular drug penetration behavior within tumor tissue after heat application, anticancer activity of anticancer drug-free liposomes and therapeutic performance using xenograft mouse models of human cancer or bigger animal models are needed prior to implementing this treatment strategy in cancer patients.

In conclusion, multifunctional liposomes facilitating tumor neovasculature-targeting and imaging, and controlled drug release at the tumor site were developed using a cRGD peptide, Gd-multi-chelate-conjugated lipid-based contrast agent, and thermosensitive block copolymer. These liposomes induced thermosensitive anticancer drug release and showed high uptake by endothelial cells expressing $\alpha_v\beta_3$ integrin. Furthermore, cRGD modification strongly favored the accumulation of liposomes at the tumor site after intravenous injection and led to remission of established solid tumors. Therefore, these multifunctional liposomes exhibit high potential as nanocarriers—with high therapeutic benefits—for use in clinical cancer therapies.

CRediT authorship contribution statement

Eiji Yuba: Conceptualization, Investigation, Methodology, Project administration, Data curation, Funding acquisition, Writing - original draft, Writing - review & editing. **Munenobu Takashima:** Investigation, Methodology. **Takaaki Hayashi:** Investigation, Methodology. **Daisuke Kokuryo:** Investigation, Methodology. **Ichio Aoki:** Data curation, Funding acquisition, Writing - review & editing. **Atsushi Harada:** Funding acquisition, Supervision, Data curation, Writing - review & editing. **Sadahito Aoshima:** Data curation, Writing - review & editing. **Uma Maheswari Krishnan:** Data curation, Writing - review & editing. **Kenji Kono:** Conceptualization, Project administration, Funding acquisition, Supervision, Data curation.

Supporting information

The Supporting Information is available free of charge on the ACS Publications website at DOI: XXX.

Table showing characterization of liposomes and Figures showing DSC analysis of liposomes, temperature-dependence of DOX release analysis for TTSL, expression

level of $\alpha_v\beta_3$ integrin on F-2 cells and colo26 cells, cellular association of TTSLs with or without cRGD, heat-triggered DOX release within cells, cytotoxicity against colon26 cells induced by DOX-loaded Polymer-lips with or without heating, cytotoxicity against F-2 cells induced by DOX-loaded TTSLs with or without heating, *ex vivo* fluorescence images of organs at 24 h after injection of ICG-loaded liposomes, immunofluoresene staining of tumor sections from the mice injected DiI-labeled liposomes, comparison of antitumor effects between Polymer-lip and Transferrin-modified Polymer-lip, and comparison of antitumor effects between cRGD-TTSL and cRGD-Polymer-lip.

Declaration of Competing Interest

The authors declare no conflict of interest.

Acknowledgements

The authors thank Kenji Kono, who was a Professor at Osaka Prefecture University and passed away at the end of 2016, for conceptualization and design of experiments, valuable discussion, and warm support. The authors thank Prof. Keiko Udaka for providing F-2 cells and Sayaka Shibata for animal experiments.

Funding: This work was supported by grants-in-aid from the Ministry of Education, Science, Sports, and Culture in Japan [26242049]; the Department of Science and Technology-Japan Society for the Promotion of Science [DST/INT/JSPS/P-221/2016]; the Japan Agency for Medical Research and Development [16cm0106202h]; and Kakenhi [17H00860]. The MRI equipment used was partly funded by the Center of Innovation Program [JPMJCE1305] of the Japan Science and Technology Agency.

Data availability statement

The data that support the findings of this study are available from the corresponding author upon reasonable request.

References

1. Xin, Y.; Yin, M.; Zhao, L.; Meng, F.; Luo, L. Recent progress on nanoparticle-based drug delivery systems for cancer therapy. *Cancer Biol. Med.* **2017**, *14*, 228–241.

2. Nakamura, Y.; Mochida, A.; Choyke, P.L.; Kobayashi, H. Nanodrug delivery: is the enhanced permeability and retention effect sufficient for curing cancer? *Bioconjug. Chem.* **2016**, *27*, 2225–2238.

3. Wilczewska, A.Z.; Niemirowicz, K.; Markiewicz, K.H.; Car, H. Nanoparticles as drug delivery systems. *Pharmacol. Rep.* **2012**, *64*, 1020–1037.

4. Maeda, H.; Wu, J.; Sawa, T.; Matsumura, Y.; Hori, K. Tumor vascular permeability and the EPR effect in macromolecular therapeutics: a review. *J. Control. Release* **2000**, *65*, 271–284.

5. Oku, N. Innovations in liposomal DDS technology and its application for the treatment of various diseases. *Biol. Pharm. Bull.* **2017**, *40*, 119–127.

6. Wan, D.; Li, C.; Pan, J. Polymeric micelles with reduction-responsive function for targeted cancer chemotherapy. *ACS Appl. Bio Mater.* **2020**, *3*, 1139–1146.

7. Fortuni, B.; Inose, T.; Ricci, M.; Fujita, Y.; Van Zundert, I.; Masuhara, A.; Fron, E.; Mizuno, H.; Latterini, L.; Rocha, S.; Uji-i, H. Polymeric engineering of nanoparticles for highly efficient multifunctional drug delivery systems. *Sci. Rep.* **2019**, *9*, 2666.

8. Minchinton, A.I.; Tannock, I.F. Drug penetration in solid tumours. *Nat. Rev. Cancer* **2006**, *6*, 583–592.

9. Trédan, O.; Galmarini, C.M.; Patel, K.; Tannock, I.F. Drug resistance and the solid tumor microenvironment. *J. Natl. Cancer Inst.* **2007**, *99*, 1441–1454.

10. Liu, D.; Yang, F.; Xiong, F.; Gu, N. The smart drug delivery system and its clinical potential, *Theranostics* **2016**, *6*, 1306–1323.

11. Lee, Y.; Thompson, D.H. 2017. Stimuli-responsive liposomes for drug delivery. *Wiley Interdiscip. Rev. Nanomed. Nanobiotechnol.* **2017**, *9*, 10.1002/wnan.1450.

12. Mura, S.; Nicolas, J.; Couvreur, P. Stimuli-responsive nanocarriers for drug delivery. *Nat. Mater.* **2013**, *12*, 991–1003.

13. Yamazaki, N.; Sugimoto, T.; Fukushima, M.; Teranishi, R.; Kotaka, A.; Shinde, C.; Kumei, T.; Sumida, Y.; Muneoka, Y.; Maruyama, K.; Yuba, E.; Harada, A.; Kono, K. Dual-stimuli responsive liposomes using pH- and temperature-sensitive polymers for controlled transdermal delivery. *Polym. Chem.* **2017**, *8*, 1507–1518.

14. Chong, J.R.; Le, D.L.; Sato, H.; Sou, K. Nanocapsule pH regulator: sustained continuous alkali release from thermosensitive liposomes reduces acid erosion. *ACS Appl. Mater. Interfaces* **2020**, *12*, 21463–21469.

15. Sou, K.; Le, D.L.; Sato, H. Nanocapsules for programmed neurotransmitter release: Toward artificial extracellular synaptic vesicles. *Small* **2019**, *15*, 1900132.

16. Le, D.L.; Ferdinandus; Tnee, C.K.; Doan, T.T.V.; Arai, S.; Suzuki, M.; Sou, K.; Sato, H. Neurotransmitter-loaded nanocapsule triggers on-demand muscle relaxation in living organism. *ACS Appl. Mater. Interfaces* **2018**, *10*, 37812–37819.

17. Zhan, J.; Lin, M.; Arai, S.; Yang, W.W.; Sou, K.; Sato, H. Electrochemical system encapsulated by nanoscale liposomes enabling on-demand triggering of electroless deposition at selected areas. *ACS Appl. Nano Mater.* **2020**, *3*, 5098–5106.

584 18. Kneidl, B.; Peller, M.; Winter, G.; Lindner, L.H.; Hossann, M. Thermosensitive liposomal
585 drug delivery systems: state of the art review. *Int. J. Nanomed.* **2014**, *9*, 4387–4398.

586 19. Affram, K.; Udofot, O.; Singh, M.; Krishnan, S.; Reams, R.; Rosenberg, J.; Agyare. E.
587 Smart thermosensitive liposomes for effective solid tumor therapy and in vivo imaging.
588 *PLoS One* **2017**, *12*, e0185116.

589 20. Kono, K. Thermosensitive polymer-modified liposomes. *Adv. Drug Deliv. Rev.* **2001**, *53*,
590 307–319.

591 21. Kono, K.; Murakami, T.; Yoshida, T.; Haba, Y.; Kanaoka, S.; Takagishi, T.; Aoshima, S.
592 Temperature sensitization of liposomes by use of thermosensitive block copolymers
593 synthesized by living cationic polymerization: effect of copolymer chain length. *Bioconjug.*
594 *Chem.* **2005**, *16*, 1367–1374.

595 22. Kono, K.; Ozawa, T.; Yoshida, T.; Ozaki, F.; Ishizaka, Y.; Maruyama, K.; Kojima, C.;
596 Harada, A.; Aoshima, S. Highly temperature-sensitive liposomes based on a thermosensitive
597 block copolymer for tumor-specific chemotherapy. *Biomaterials* **2010**, *31*, 7096–7105.

598 23. Kono, K.; Takashima, M.; Yuba, E.; Harada, A.; Hiramatsu, Y.; Kitagawa, H.; Otani, T.;
599 Maryama, K.; Aoshima, S. Multifunctional liposomes having target specificity, temperature-
600 triggered release, and near-infrared fluorescence imaging for tumor-specific
601 chemotherapy. *J. Control. Release* **2015**, *216*, 69-77.

602 24. Danhier, F.; Le Breton, A.L.; Préat, V. RGD-based strategies to target alpha(v) beta(3)
603 integrin in cancer therapy and diagnosis. *Mol. Pharm.* **2012**, *9*, 2961–2973.

604 25. Smith, B.R.; Cheng, Z.; De, A.; Rosenberg, J.; Gambhir, S.S. Dynamic visualization of
605 RGD-quantum dot binding to tumor neovasculature and extravasation in multiple living
606 mouse models using intravital microscopy. *Small* **2010**, *6*, 2222–2229.

607 26. Quader, S.; Liu, X.; Chen, Y.; Mi, P.; Chida, T.; Ishii, T.; Miura, Y.; Nishiyama, N.; Cabral,
608 H.; Kataoka, K. cRGD peptide-installed epirubicin-loaded polymeric micelles for effective
609 targeted therapy against brain tumors. *J. Control. Release* **2017**, *258*, 56–66.

610 27. Zhang, Y.; Pan, J.; Xu, Q.; Li, H.; Wang, J.; Zhang, C.; Hong, G. Synthesis and in vitro
611 experiments of carcinoma vascular endothelial targeting polymeric nano-micelles combining
612 small particle size and supermagnetic sensitivity. *Int. J. Med. Sci.* **2018**, *15*, 498–506.

613 28. Song, Z.; Lin, Y.; Zhang, X.; Feng, C.; Lu, Y.; Gao, Y.; Dong, C. Cyclic RGD peptide-
614 modified liposomal drug delivery system for targeted oral apatinib administration: enhanced
615 cellular uptake and improved therapeutic effects. *Int. J. Nanomed.* **2017**, *12*, 1941–1958.

616 29. Kono, K.; Nakashima, S.; Kokuryo, D.; Aoki, I.; Shimomoto, H.; Aoshima, S.; Maruyama,
617 K.; Yuba, E.; Kojima, C.; Harada, A.; Ishizaka, Y. Multi-functional liposomes having
618 temperature-triggered release and magnetic resonance imaging for tumor-specific
619 chemotherapy. *Biomaterials* **2011**, *32*, 1387–1395.

620 30. Bulbake, U.; Doppalapudi, S.; Kommineni, N.; Khan, W. Liposomal formulations in clinical
621 use: an updated review. *Pharmaceutics* **2017**, *9*, 12.

622 31. Needham, D.; Anyarambhatla, G.; Kong, G.; Dewhirst, M.W. A new temperature-sensitive
623 liposome for use with mild hyperthermia: characterization and testing in a human tumor
624 xenograft model. *Cancer Res.* **2000**, *60*, 1197–1201.

625 32. Yatvin, M.B.; Weinstein, J.N.; Dennis, W.H.; Blumenthal, R. Design of liposomes for
626 enhanced local release of drugs by hyperthermia. *Science* **1978**, *202*, 1290–1293.

627 33. Kong, G.; Anyarambhatia, G.; Petros, W.P.; Braun, R.D.; Colvin, O.M.; Needham, D.;
628 Dewhirst, M.W. Efficacy of liposomes and hyperthermia in a human tumor xenograft model:
629 importance of triggered drug release. *Cancer Res.* **2000**, *60*, 6950–6957.

630 34. Toda, K.; Tsujioka.; K, Maruguchi, Y.; Ishii, K.; Miyachi, Y.; Kuribayashi, K.; Imamura, S.
631 Establishment and characterization of a tumorigenic murine vascular endothelial cell line (F-
632 2). *Cancer Res.* **1990**, *50*, 5526–5530.

633 35. Kokuryo, D.; Nakashima, S.; Ozaki, F.; Yuba, E.; Chuang, K.H.; Aoshima, S.; Ishizaka, Y.;
634 Saga, T.; Kono, K.; Aoki, I. Evaluation of thermo-triggered drug release in intramuscular-
635 transplanted tumors using thermosensitive polymer-modified liposomes and MRI.
636 *Nanomedicine* **2015**, *11*, 229–238.

637 36. Aoki, I.; Yoneyama, M.; Hirose, J.; Minemoto, Y.; Koyama, T.; Kokuryo, D.; Bakalova, R.;
638 Murayama, S.; Saga, T.; Aoshima, S.; Ishizaka, Y.; Kono, K. Thermoactivatable polymer-
639 grafted liposomes for low-invasive image-guided chemotherapy. *Transl. Res.* **2015**, *166*,
640 660–673.

641 37. Lugano, R.; Ramachandran, M.; Dimberg, A. Tumor angiogenesis: causes, consequences,
642 challenges and opportunities. *Cell Mol. Life Sci.* **2020**, *77*, 1745–1770.
643

For Table of Contents Use Only

Multifunctional traceable liposomes with temperature-triggered drug release and neo-vasculature targeting properties for improved cancer chemotherapy

Eiji Yuba[1]*, Munenobu Takashima[1], Takaaki Hayashi[1], Daisuke Kokuryo[2,3], Ichio Aoki[3], Atsushi Harada[1], Sadahito Aoshima[4], Uma Maheswari Krishnan[5], Kenji Kono[1]